

## Investigating the large deformation of the $5/2^+$ isomeric state in $^{73}\text{Zn}$ : An indicator for triaxiality

X. F. Yang,<sup>1,2,\*</sup> Y. Tsunoda,<sup>3</sup> C. Babcock,<sup>4</sup> J. Billowes,<sup>5</sup> M. L. Bissell,<sup>5</sup> K. Blaum,<sup>6</sup> B. Cheal,<sup>4</sup> K. T. Flanagan,<sup>5,7</sup> R. F. Garcia Ruiz,<sup>5</sup> W. Gins,<sup>2</sup> C. Gorges,<sup>8,9</sup> L. K. Grob,<sup>10,9</sup> H. Heylen,<sup>10</sup> S. Kaufmann,<sup>9</sup> M. Kowalska,<sup>10</sup> J. Krämer,<sup>9</sup> S. Malbrunot-Ettenauer,<sup>10</sup> R. Neugart,<sup>6,8</sup> G. Neyens,<sup>2,10</sup> W. Nörtershäuser,<sup>9</sup> T. Otsuka,<sup>11,3,12,2,13</sup> J. Papuga,<sup>2</sup> R. Sánchez,<sup>14</sup> C. Wraith,<sup>4</sup> L. Xie,<sup>5</sup> and D. T. Yordanov<sup>15</sup>

<sup>1</sup>*School of Physics and State Key Laboratory of Nuclear Physics and Technology, Peking University, Beijing 100871, China*

<sup>2</sup>*Instituut voor Kern- en Stralingsfysica, KU Leuven, B-3001 Leuven, Belgium*

<sup>3</sup>*Center for Nuclear Study, University of Tokyo, Hongo, Bunkyo-ku, Tokyo 113-0033, Japan*

<sup>4</sup>*Oliver Lodge Laboratory, Oxford Street, University of Liverpool, Liverpool L69 7ZE, United Kingdom*

<sup>5</sup>*School of Physics and Astronomy, The University of Manchester, Manchester M13 9PL, United Kingdom*

<sup>6</sup>*Max-Planck-Institut für Kernphysik, D-69117 Heidelberg, Germany*

<sup>7</sup>*Photon Science Institute Alan Turing Building, University of Manchester, Manchester M13 9PY, United Kingdom*

<sup>8</sup>*Institut für Kernchemie, Universität Mainz, D-55128 Mainz, Germany*

<sup>9</sup>*Institut für Kernphysik, TU Darmstadt, D-64289 Darmstadt, Germany*

<sup>10</sup>*Experimental Physics Department, CERN, CH-1211 Geneva 23, Switzerland*

<sup>11</sup>*Department of Physics, University of Tokyo, Hongo, Bunkyo-ku, Tokyo 113-0033, Japan*

<sup>12</sup>*RIKEN Nishina Center, 2-1 Hirosawa, Wako, Saitama 351-0198, Japan*

<sup>13</sup>*National Superconducting Cyclotron Laboratory, Michigan State University, East Lansing, Michigan 48824, USA*

<sup>14</sup>*GSI Helmholtzzentrum für Schwerionenforschung, D-64291 Darmstadt, Germany*

<sup>15</sup>*Institut de Physique Nucléaire, CNRS-IN2P3, Université Paris-Sud, Université Paris-Saclay, 91406 Orsay, France*



(Received 23 March 2018; published 30 April 2018)

Recently reported nuclear spins and moments of neutron-rich Zn isotopes measured at ISOLDE-CERN [C. Wraith *et al.*, *Phys. Lett. B* **771**, 385 (2017)] show an uncommon behavior of the isomeric state in  $^{73}\text{Zn}$ . Additional details relating to the measurement and analysis of the  $^{73m}\text{Zn}$  hyperfine structure are addressed here to further support its spin-parity assignment  $5/2^+$  and to estimate its half-life. A systematic investigation of this  $5/2^+$  isomer indicates that significant collectivity appears due to proton/neutron  $E2$  excitations across the proton  $Z = 28$  and neutron  $N = 50$  shell gaps. This is confirmed by the good agreement of the observed quadrupole moments with large scale Monte Carlo shell model calculations. In addition, potential energy surface calculations in combination with T plots reveal a triaxial shape for this isomeric state.

DOI: [10.1103/PhysRevC.97.044324](https://doi.org/10.1103/PhysRevC.97.044324)

### I. INTRODUCTION

Transitional regions of the nuclear chart often attract significant interest. They usually bridge several different aspects of nuclear structure, such as single-particle properties, configuration mixing, nucleon-nucleon (NN) correlations, as well as collective behavior. One region lying “northeast” of  $^{68}\text{Ni}$ , where structural changes occur suddenly, has been the subject of extensive experimental and theoretical investigations in recent years. A subshell closure effect at  $N = 40$  was long suggested in Ni from the experimentally observed high-lying first  $2^+$  level and a local minimum in the  $B(E2; 0^+ \rightarrow 2^+)$  value in  $^{68}\text{Ni}$  [1,2]. High-precision mass measurements revealed evidence for only a very weak subshell closure at  $^{68}\text{Ni}$ , which disappears

quickly when moving away from  $Z = 28$  [3,4]. Collectivity effects appear with only two neutrons/protons above  $N = 40$ ,  $Z = 28$ , and a maximum is found at  $N = 42$  in the even-even systems (Zn, Ge, and Se) as indicated by  $B(E2; 0^+ \rightarrow 2^+)$  and  $E(2^+)$  measurements [5–8]. Various nuclear shapes are also found in this region, in particular for Ge and Se isotopes, such as the well-known shape coexistence and triaxial shapes [9–11]. An unusual triaxial shape has also been proposed for  $^{72}\text{Zn}$  [12,13].

Measurements of ground state properties from laser spectroscopy have also provided considerable nuclear structure information in this region [14–19]. With one proton above  $Z = 28$ , a study of Cu isotopes revealed a primarily single-particle nature and a weak “magic” behavior around  $N = 40$  from the spins, moments, and charge radii, but also showed a non-negligible contribution from NN correlations and cross-shell excitations [14,16,17]. In contrast, with two and three protons above  $Z = 28$ , the collective behavior above  $N > 40$  is significantly enhanced in the Zn and Ga isotopic chains, as indicated by their measured quadrupole moments [15,19]. It was concluded in Ref. [19] that Zn isotopes are considered

\* xiaofei.yang@pku.edu.cn

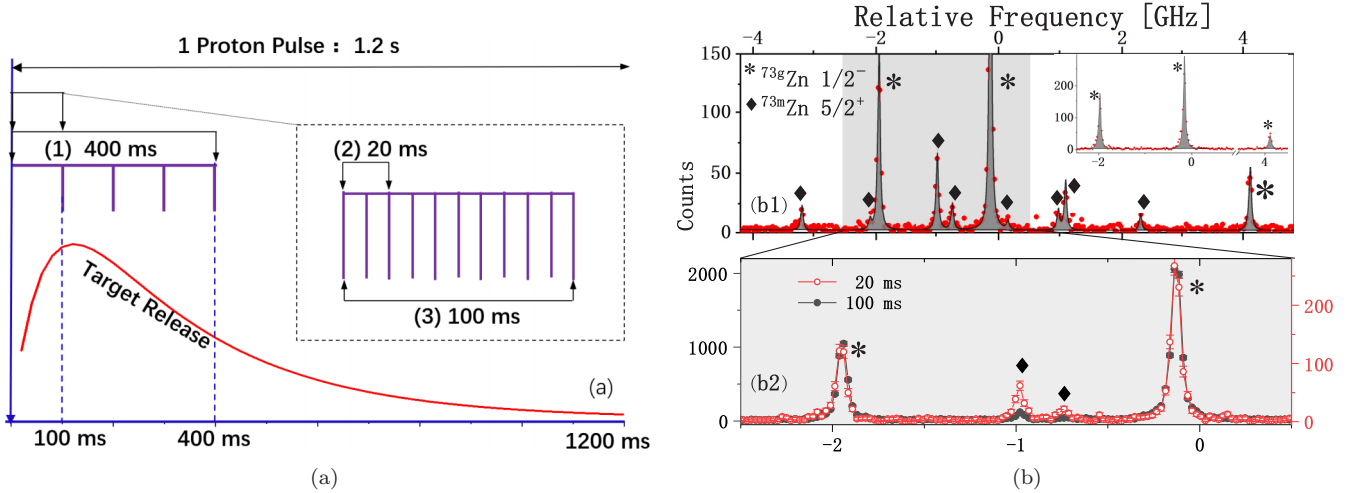


FIG. 1. (a) Three different timings used for ion accumulation and measurement are shown relative to the release time of Zn from the target. In (1), ions were collected for 400 ms (consisting of four 100 ms accumulation and release cycles in ISCOOL) after each proton pulse, yielding only the  $1/2^-$  ground state structure [(b1) inset]. In (2), only the ions released from the target in the first 20 ms (two 10 ms cycles) are used, revealing the  $5/2^+$  isomer peaks (b1) labeled with diamonds. In (3), the measurement period is extended to 100 ms (of ten 10 ms cycles), which reduces the isomeric count rate relative to the ground state (b2).

to lie within a transitional region between spherical Ni and deformed Ge nuclei.

In recent laser spectroscopy studies on neutron-rich Zn isotopes ( $^{69-79}\text{Zn}$ ), several earlier observed isomeric states were identified in all odd-Zn isotopes, and spins and parities could be unambiguously assigned [19]. However, no evidence was seen for a long-lived (5.8 s) isomeric state in  $^{73}\text{Zn}$ , which had been proposed to exist in  $^{73}\text{Zn}$ , from a  $\beta$ -decay study on a cocktail beam of  $A = 73$  isotopes [20]. Such a long-lived isomer was not seen, however, in the  $\beta$  decay of a  $^{73}\text{Cu}$  beam produced in projectile fragmentation [21]. The latter work proposed a 13 ms isomeric state to exist in  $^{73}\text{Zn}$  with a tentative spin-parity assignment of  $5/2^+$  at 195 keV. The lifetime and decay energy of this isomeric state were also confirmed in a recent  $\beta$ -decay study of a  $^{73}\text{Zn}$  beam produced via laser ionization [22]. Thus, the existence of a 5.8 s isomer and its decaying transitions remains unconfirmed.

In this article, additional information for the laser spectroscopy measurement and for the analysis of  $^{73g,m}\text{Zn}$  is provided to estimate the half-life of the observed isomer and to firmly assign spin  $5/2$  and positive parity. We also want to establish or to eliminate simultaneously the possible existence of an additional long-lived isomer, having a 5.8 s half-life. The magnetic and quadrupole moments of the  $5/2^+$  isomeric state were reported in our prior work [19], where the results were compared to large scale shell model calculations with different effective interactions. Here we provide further analysis of the wave function of the isomeric state obtained through shell model calculations [23,24] with two effective interactions. We also present potential energy surface (PES) calculations and T plots [24,25], giving insight into the shape of the isomer and other states in this region.

## II. EXPERIMENTAL DETAILS

The experiment was performed at the collinear laser spectroscopy (COLLAPS) setup [26] at CERN-ISOLDE, as de-

tailed in earlier publications [18,19]. The Zn isotopes were produced by impinging 1.4-GeV protons onto a neutron converter [27] of a  $\text{UC}_x$  target, laser resonantly ionized by the resonant ionization laser-ion source [28], and accelerated up to 30 keV. The ions of interest were cooled and bunched in a gas-filled radio-frequency quadrupole (ISCOOL) [29] after mass separation by the high-resolution separator (HRS), and then delivered into the COLLAPS setup. After a charge exchange process with Na vapor, the neutralized Zn atoms were resonantly excited by a cw frequency-doubled Ti:sapphire laser with the wavelength matching the  $4s4p\ ^3P_2 \rightarrow 4s5s\ ^3S_1$  transition. A tuning voltage applied to the charge exchange cell was used to Doppler shift the laser frequency over the range of the hyperfine resonances of Zn atoms. The emitted fluorescence photons from the laser excited atoms were recorded by four photomultiplier tubes as a function of the scanning voltage to obtain the hyperfine structure (HFS) spectra of the Zn isotopes. More detailed descriptions of the experimental setup and measurement method can be found in [19], which discusses the nuclear spins, magnetic moments and quadrupole moments of  $^{63-79}\text{Zn}$  isotopes.

Here we focus on the HFS measurement process for the  $^{73}\text{Zn}$  isotope, where we used three different measurement procedures to distinguish the presence of isomeric states with different lifetimes. Thanks to the relatively fast release [30] of Zn from the target [red curve in Fig. 1(a)], a total measurement time after each proton pulse (every 1.2 s) could be limited to 400 ms. The laser-ionized mass  $A = 73$  beam was accumulated in the ISCOOL buncher for 100 ms and released in a few microseconds, a process that was repeated four consecutive times after each proton pulse; see Fig. 1(a). Under this measurement condition, the typical hyperfine spectrum (HFS) obtained for  $^{73}\text{Zn}$  is shown in the small inset of Fig. 1(b1). Three resonances were observed in a total measurement range of  $>5$  GHz, confirming a nuclear spin of  $I = 1/2$  for the ground state ( $T_{1/2} = 23.5$  s [31]). A long-lived (5.8 s) isomer

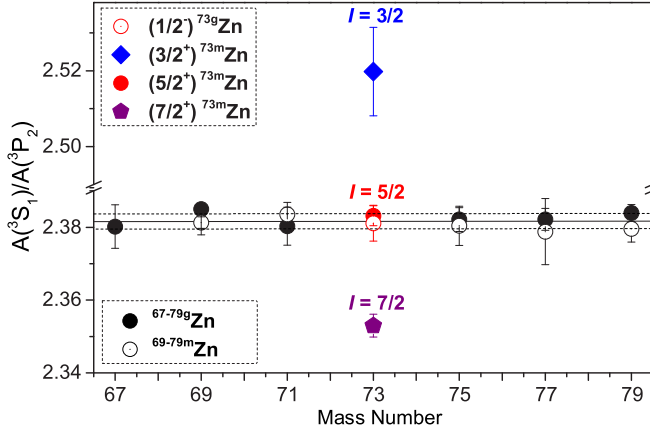


FIG. 2. Ratio between the hfs constants  $A(^3S_1)$  and  $A(^3P_2)$ . The continuous and dashed lines show the average value of  $A(^3S_1)/A(^3P_2) = 2.3817(19)$ . The hyperfine spectra of  $^{73m}\text{Zn}$  were fitted by assuming different spins,  $I = 3/2, 5/2, 7/2$ .

with higher spin as proposed in [20] was not observed in the current spectrum, indicating that it does not exist or is not populated with this reaction in the target. However, since positive parity high-spin states in  $^{69,71,75,77,79}\text{Zn}$  were easily observed under the same experimental conditions [18,19], we conclude that there is no evidence of a 5.8 s isomeric state in  $^{73}\text{Zn}$ . To be able to observe any short-lived isomer and enhance the total production of  $^{73}\text{Zn}$ , the 1.4-GeV proton beam was switched to impinge directly on the  $\text{UC}_x$  target instead of a neutron converter. To enhance the resonance signal of a short-lived isomer relative to the ground state, the measurement period was reduced to only 20 ms following each proton pulse, consisting of 2 accumulation cycles of 10 ms each in ISCOOL [timing (2) in Fig. 1(a)]. Additional new resonances [Fig. 1(b1)] were observed by using these particular settings, confirming the existence of a short-lived isomer. By extending the measurement time to 100 ms after the proton pulse, as shown with timing (3) in Fig. 1(a), the relative intensity of the highest peak for the isomer is reduced by a factor of 5 compared to that of the ground state, as shown in Fig. 1(b2). This confirms the isomer half-life to be of the order of 10 ms, thus consistent with the isomer observed in the previous studies [21,22].

The HFS of the  $^{73m}\text{Zn}$  was carefully analyzed by using a  $\chi^2$ -minimization technique (commonly used for HFS analysis [32]) with different assumptions of the isomeric spin, but only spin 5/2 can reproduce all resonance peaks with a reasonable reduced  $\chi^2$  ( $\sim 1.04$ ). The HFS constants,  $A$ ,  $B$ , for both  $4s4p\ ^3P_2$  and  $4s5s\ ^3S_1$  states can be obtained from this analysis procedure, as explained in [19]. To further support the spin assignment, we verified the ratio of the magnetic HFS constant for the two atomic states,  $R = A(^3S_1)/A(^3P_2)$ , with different spin assumptions ( $I = 3/2, 5/2, 7/2$ ). If a correct spin is assumed, then  $R$  should be a constant over the entire isotopic chain (neglecting a possible small hyperfine anomaly). As shown in Fig. 2, only with the spin 5/2 assumption is the  $R$  value consistent with those from the other isotopes, thus establishing firmly a spin 5/2 assignment to  $^{73m}\text{Zn}$  [19]. The positive parity has already been confirmed by the reported magnetic moment [19].

TABLE I. Experimental quadrupole moments of the long-lived high-spin states in  $^{69-79}\text{Zn}$  [19] compared to JUN45 and A3DA-m shell model calculations.

| $A$    | $I^\pi$ | $Q_{\text{exp}}$ (b) | $Q_{\text{JUN45}}$ (b) | $Q_{\text{A3DA-m}}$ (b) |
|--------|---------|----------------------|------------------------|-------------------------|
| $69^m$ | $9/2^+$ | $-0.39(3)$           | $-0.41$                | $-0.435$                |
| $71^m$ | $9/2^+$ | $-0.26(3)$           | $-0.284$               | $-0.264$                |
| $73^m$ | $5/2^+$ | $+0.43(4)$           | $+0.281$               | $+0.42$                 |
| $75$   | $7/2^+$ | $+0.16(2)$           | $+0.07$                | $+0.055$                |
| $77$   | $7/2^+$ | $+0.48(4)$           | $+0.421$               | $+0.487$                |
| $79$   | $9/2^+$ | $+0.40(4)$           | $+0.356$               | $+0.367$                |

### III. INTERPRETATIONS OF EXPERIMENTAL QUADRUPOLE MOMENTS

Some of the experimental spins and quadrupole moments for neutron-rich Zn isotopes are summarized in Table I. As discussed in [19], all ground and isomeric state magnetic and quadrupole moments can be explained as being due to one or more unpaired neutrons in one particular orbital, except for the moments of  $^{73m}\text{Zn}$ . In a simple shell model picture, as the neutrons fill the  $\nu g_{9/2}$  orbit, an unpaired neutron results in a spin of  $9/2^+$ , and possibly spins  $7/2^+$  or  $5/2^+$  can be obtained from a seniority-3 configuration [33]. Therefore, the  $g$  factor of these states should follow the effective  $g$  factor of neutrons in a  $\nu g_{9/2}$  orbit, which is indeed true for all high-spin isotopes/isomers except for the  $5/2^+$  isomer of  $^{73}\text{Zn}$ . Similarly, the quadrupole moments of  $9/2^+$  and  $7/2^+$  states can be easily accounted for by a standard calculation with seniorities 1 and 3 for one and three unpaired particles in the  $\nu g_{9/2}$  orbit, while the  $5/2^+$  isomer reveals a significantly larger positive value contrary to the expected small positive quadrupole moment for seniority 3 ( $\nu 1g_{9/2}$ ) $_{I=5/2^+}^3$  (see Fig. 3).

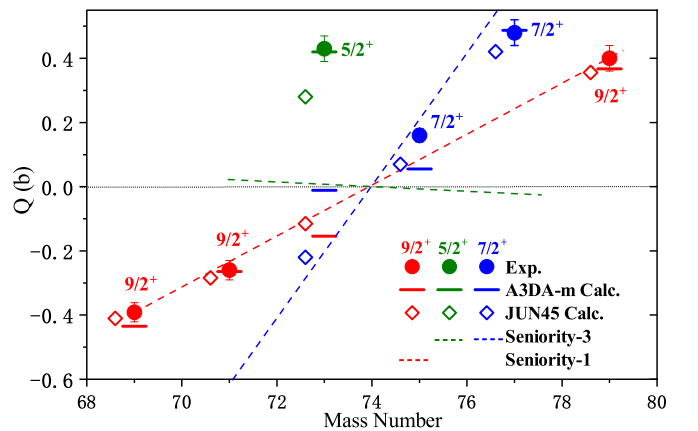


FIG. 3. Experimental  $Q$  moments of high-spin states of  $^{69-79}\text{Zn}$  compared with the shell model calculation using JUN45 (open diamonds) and A3DA-m interactions (solid lines), and the expected values (dashed lines) for a seniority-1 ( $g_{9/2}$ ) $^n$  configuration and the spin  $7/2^+$  and  $5/2^+$  seniority-3 configurations. Note that the data points for the JUN45 calculation have been shifted to the left slightly to avoid any overlap.

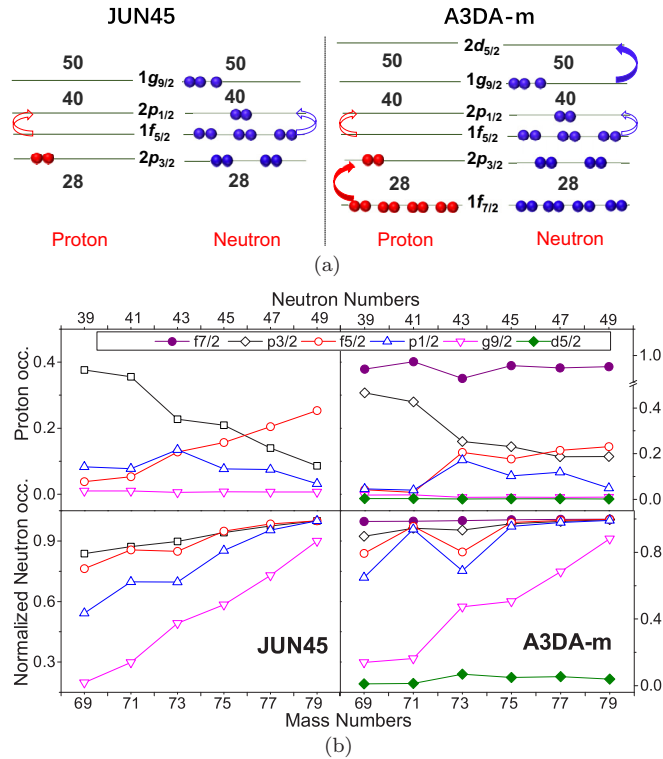


FIG. 4. (a) Model spaces for the JUN45 and A3DA-m shell model interactions. (b) Normalized proton/neutron occupancies in different orbits for the high-spin states of  $^{69-79}\text{Zn}$  calculated by JUN45 and A3DA-m interactions.

### A. Tracking the source of collectivity

Shell model calculations using two different effective shell-model interactions, JUN45 in a proton/neutron  $pf_{5/2}g_{9/2}$  model space and A3DA-m in a  $fp_{g_{9/2}}d_{5/2}$  model space, as shown in Fig. 4(a), were used to investigate the spins and the magnetic and quadrupole moments of  $^{69-79}\text{Zn}$  [19]. While overall the agreement between calculated and experimental quadrupole moments is better with the A3DA-m interaction (Table I), the large quadrupole moment of the  $^{73}\text{Zn}$  isomer is only reproduced by using the A3DA-m interaction, which includes proton and neutron excitations across  $Z = 28$  and  $N = 50$  (Fig. 3). These calculations also provide the proton/neutron occupancies in different orbits of the entire model space, as shown in Fig. 4(b). Note that the occupations of proton and neutrons are normalized to the total allowed occupancy ( $2j + 1$ ) of each orbit. A relative occupancy of 1 represents a fully occupied orbit. Results from both interactions show a clear inversion of the proton occupation from the  $\pi p_{3/2}$  (open black squares) to  $\pi f_{5/2}$  (open red circles) orbits between  $N = 45$  and  $N = 47$ . From the moments measured in Cu ( $Z = 29$ ), this inversion was shown to occur between  $N = 43$  and  $N = 45$  ( $^{75}\text{Cu}$ ) [14] and in the Ga ( $Z = 31$ ) isotopes it occurs between  $N = 47$  and  $N = 49$  ( $^{79}\text{Ga}$ ) [15]. This is attributed to the monopole effect of the tensor force, first proposed by Otsuka *et al.* [34,35]. For the JUN45 calculations, a gradual increase of the neutron occupations in all neutron orbits is observed as neutrons are added to the  $g_{9/2}$  orbit.

Calculations using A3DA-m show a sudden decrease in the neutron  $f_{5/2}$  and  $p_{1/2}$  occupation probabilities at mass 73, in favor of an increase in the neutron  $d_{5/2}$  occupation. At the same time, a decrease in the proton  $f_{7/2}$  occupation is seen. The sudden change in the proton  $f_{7/2}$  and neutron  $d_{5/2}$  occupations in the  $^{73}\text{Zn}$  isomeric wave function is needed to reproduce the large observed quadrupole moment. It illustrates that in  $^{73m}\text{Zn}$  a certain degree of proton excitations across the closed  $Z = 28$  shell and neutron excitations across the  $N = 50$  shell gaps are important. This was also observed recently in the neutron-rich Cu isotopes via mass and moment measurements [17,36]. The most noteworthy conclusion from Fig. 4(b) is the overall “kink” in the proton and neutron level occupations at  $N = 43$ , corresponding to the  $5/2^+$  isomer of  $^{73}\text{Zn}$ . It indicates a significantly enhanced admixture in the wave function of the  $5/2^+$  state. This observation is consistent with the earlier observed enhanced collectivity around  $N = 42$  in the even-even Zn, Ge, and Se isotopes [5–8,12].

As mentioned above and illustrated in Fig. 3, a small positive value is expected for the quadrupole moment of the  $5/2^+$  state from a simple calculation of seniority 3 (green dashed line), while calculations with the JUN45 interaction and especially with the A3DA-m interaction predict a large positive quadrupole moment, much closer to the experimental result. A further investigation under different shell model truncations illustrates that the large positive quadrupole moment can only be obtained when  $E2$  excitations of both protons and neutrons are allowed [as marked with the open arrows in Fig. 4(a)]. From this perspective, a larger quadrupole moment will be expected naturally from the shell model calculation in a large model space by using the A3DA-m interaction. Figure 4(b) shows that both proton excitation across  $Z = 28$  and neutron excitation across  $N = 50$  (both of  $E2$  type) are indeed enhanced for the case of the  $5/2^+$  state of  $^{73}\text{Zn}$ . As a result, the A3DA-m calculation shows an excellent agreement with the experimental value for the abnormally large quadrupole moment of the  $5/2^+$  state in  $^{73}\text{Zn}$  (See Fig. 3 and Table I).

Another notable feature of Fig. 3 is that, for the  $7/2^+$  and  $9/2^+$  states in  $^{73}\text{Zn}$ , the predictions using the JUN45 interaction (open symbols) match nicely the trend from seniorities 1 and 3 (dashed lines). However, with A3DA-m interaction, only the calculated  $9/2^+$  quadrupole moment follows approximately the trend for seniority 1, while the calculated quadrupole moment for the  $7/2^+$  deviates significantly from the seniority-3 trend line, as well as that for  $5/2^+$  state in  $^{73}\text{Zn}$ . An explanation for this is given in the next paragraph, based on a T-plot analysis.

### B. Triaxial shape

As the A3DA-m interaction in the Monte Carlo shell model (MCSM) framework nicely reproduces the experimental quadrupole moments of the high-spin states in  $^{71-79}\text{Zn}$  (Fig. 3), and especially that of  $^{73m}\text{Zn}$ , it makes sense to investigate further the shapes of these different states by using the T plot, which is a method to analyze the MCSM wave function, as detailed in Refs. [24,25]. By using the MCSM calculations, a set of Slater determinants called MCSM basis vectors are generated. For each MCSM basis vector,

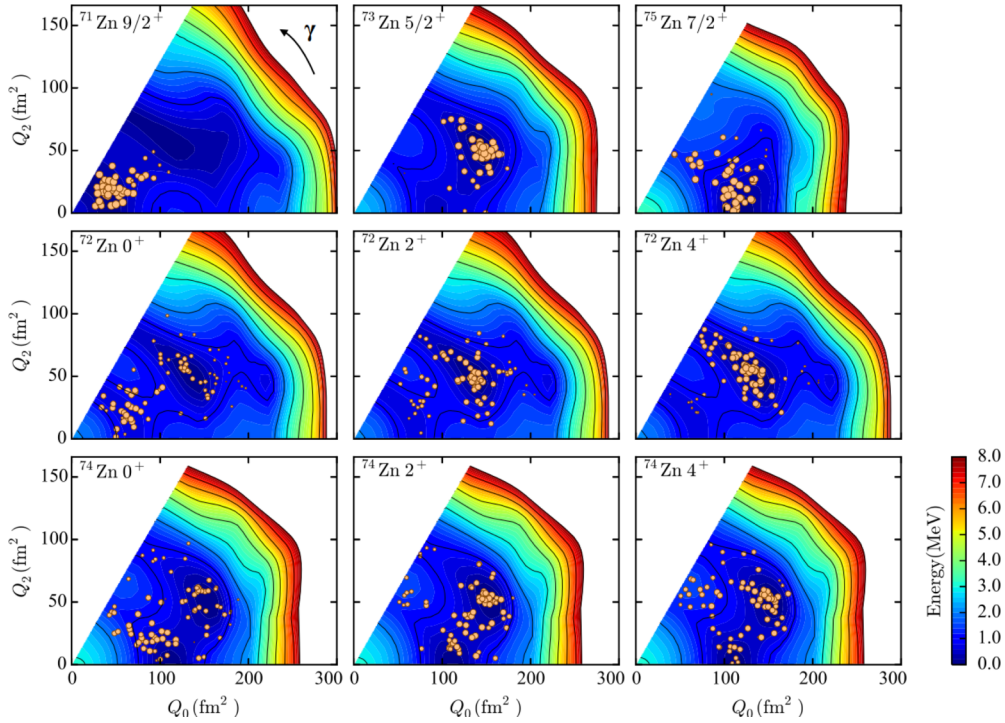


FIG. 5. Potential energy surfaces (PES) of high-spin states in  $^{71-75}\text{Zn}$  isotopes and  $0^+$ ,  $2^+$ , and  $4^+$  states of  $^{72,74}\text{Zn}$ , coordinated by  $Q_0$  and  $Q_2$  calculated using MCSM. The distribution of the MCSM basis states is depicted by the circles. The locations of the circles indicate the intrinsic shapes of the MCSM basis states and the sizes denote their importance in the total wave function; see Ref. [24] for more information.

the intrinsic quadrupole moments,  $Q_0 \propto \langle 2z^2 - x^2 - y^2 \rangle$  and  $Q_2 \propto \langle x^2 - y^2 \rangle$ , can be calculated. Each basis vector can then be identified by a circle on the potential energy surface (PES), where the intrinsic quadrupole moments are the coordinates, as shown in Fig. 5. The sizes of the circles reflect the overlap probability of each MCSM basis vector with the eigenstate, and thus depicts the importance of each basis vector in the total wave function. In other words, the size of the circle on the PES visualizes the shape information of the MCSM basis vector and its importance for a given eigenstate, while the distribution of the circles represents the distribution of MCSM basis vectors indicating the intrinsic quadrupole moments of a given state. Therefore, by using the T-plot method, the intrinsic shape of a given state can be easily determined by analyzing the distribution and size of MCSM basis states (circles on the PES).

In the upper row of Fig. 5, we compare the T plot for the  $5/2^+$  state in  $^{73}\text{Zn}$  to that of the high-spin states in  $^{71,75}\text{Zn}$ . The MCSM basis vectors of the  $9/2^+$  isomeric state of  $^{71}\text{Zn}$ , with one single neutron in the  $\nu g_{9/2}$  orbit, are distributed around a limited region of spherical shape. This is consistent with its single-particle nature, as confirmed from its  $g$  factor and quadrupole moment [19]. With an additional four neutrons added to the  $\nu g_{9/2}$  orbit, a moderately prolate shape is suggested for the  $7/2^+$  state in  $^{75}\text{Zn}$ , consistent with the measured positive quadrupole moment for this seniority-3 configuration. As for the  $5/2^+$  state in  $^{73}\text{Zn}$ , the MCSM basis vectors are depicted with relatively large circles and are all concentrated on an energy minimum at  $\gamma \sim 30^\circ$ , indicating a triaxial shape for this state.

It is also worth verifying the shapes of the first  $0^+$ ,  $2^+$ ,  $4^+$  states in the adjacent even-even isotopes ( $^{72,74}\text{Zn}$ ), as triaxiality is also proposed for  $^{72}\text{Zn}$  by Coulomb excitation and reaction experiments [12,13]. Indeed, triaxiality is most pronounced in the  $4^+$  state in  $^{72}\text{Zn}$ , while the diffused MCSM basis vectors in the other levels point to shape fluctuations.

Although it has been the subject of numerous experimental investigations in this region, detailed spectroscopic information for the mid-shell isotope  $^{73}\text{Zn}$  remains inconclusive [20–22,37]. Here, we may further compare available states of  $^{73}\text{Zn}$  with those calculated using the shell model. Figure 6(a) summarizes the very limited experimental information (energies, spins, and parities) and the corresponding states predicted by the MCSM using the A3DA-m interaction. Within the typical uncertainty for the energy as calculated by the shell model (about a few 100 keV), the A3DA-m interaction provides the correct order of long-lived states in  $^{73}\text{Zn}$ . Note that, as discussed in [19], the JUN45 shell model interaction cannot predict the correct order of ground and isomeric states for  $^{73}\text{Zn}$ . Furthermore, the possible shapes of all given states in  $^{73}\text{Zn}$  can be investigated by using the T plot obtained from MCSM calculations, as seen in Fig. 6(b). Here we only present the result for one negative parity state, the  $1/2^-$  ground state of  $^{73}\text{Zn}$ , showing a considerable shape fluctuation with a wide distribution of the MCSM basis vectors towards a moderate prolate shape. Apart from the noticeable spread of MCSM basis vectors and the corresponding shape fluctuations for the first  $9/2^+$  state, all other positive parity states have a focused distribution of basis vectors around  $\gamma \sim 30^\circ$ , pointing to triaxial shapes for all these levels. The first  $9/2^+$  state is

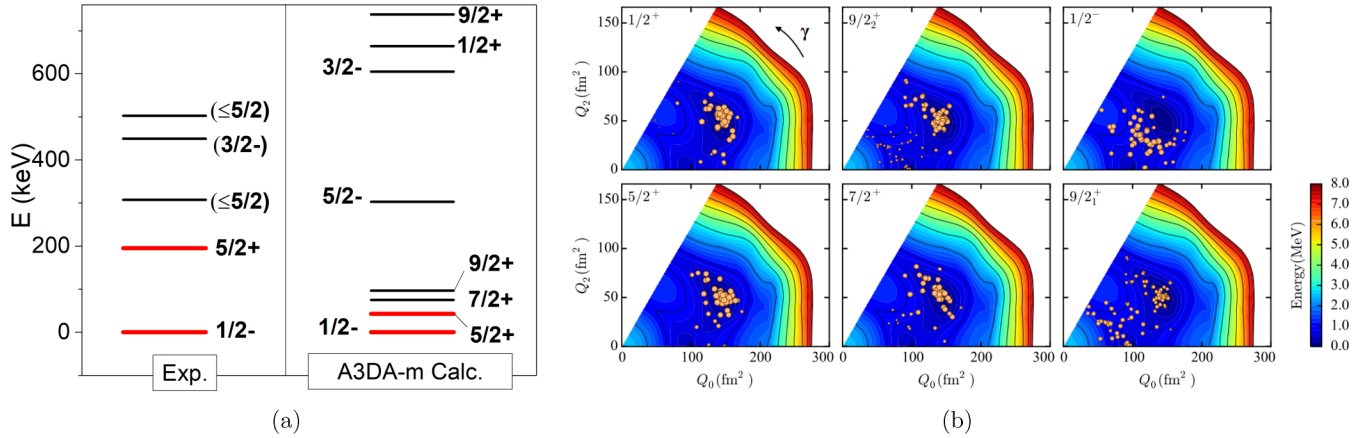


FIG. 6. (a) Experimentally observed energy levels compared with those calculated by MCSM, and (b) the T plots of these states in  $^{73}\text{Zn}$ .

considered a mixture of a spherical shape with some triaxial components, as seen from its T plot. This explains why the calculated quadrupole moment for the  $9/2^+$  state in  $^{73}\text{Zn}$  roughly follows the simple picture of seniority, while results for  $7/2^+$  and  $5/2^+$  states have pronounced deviations, as discussed above for Fig. 3.

Triaxiality has been the subject of investigation in the nearby isotopic chains of Ge and Se [38–41], and is also suggested for adjacent even-even  $^{72}\text{Zn}$  [12, 13], although it has not previously been known to exist in  $^{73}\text{Zn}$ . Experimental evidence for triaxial deformation is usually provided by  $\gamma$ -ray spectroscopy, as in the even-even isotopes  $^{74,76}\text{Ge}$  ( $Z = 32$ ) [9, 10], odd-odd  $^{74}\text{As}$  ( $Z = 33$ ) [42], and  $^{75}\text{Se}$  ( $Z = 34$ ) [11].

Analogously, another region where the  $5/2^+$  state originates from the three quasiparticle configuration of  $\pi(1g_{9/2})^3_{I=5/2^+}$  is near  $Z \approx 43$ , including, for example, the isotopes  $^{99,101,103}\text{Y}$ ,  $^{101,103,105}\text{Nb}$ , and  $^{109,111}\text{Tc}$ . Laser spectroscopy has been performed on exotic Y and Nb isotopes, resulting in quadrupole moments for  $5/2^+$  states larger by a factor of 2 ( $^{99,101}\text{Y}$  and  $^{101,103}\text{Nb}$ ) than the normal  $9/2^+$  state [43, 44]. These isotopes happen to lie within a region of shape transition around  $N = 60$ , which has been confirmed by a sudden increase of collectivity, as concluded from complementary observables [radii,  $S_{2n}$ ,  $E(2^+)$ ] and theoretical predictions [25, 45–47]. However, a detailed analysis of the level schemes in the Y and Nb isotopes and theoretical analysis of other isotopes in the region also point to triaxiality in the Tc and Rh isotopes [48], which seems to be similar to nuclei near  $N \approx 43$ . It is essential to have further experimental and theoretical investigations in these regions, such as laser spectroscopy measurements of Ge, Se, and Tc isotopes, to pin down the connection between the deformation and triaxiality, and to eventually have a better understanding of the shape of the  $5/2^+$  isomer in  $^{73}\text{Zn}$ .

#### IV. SUMMARY

Additional experimental information relating to our  $^{73}\text{Zn}$  hyperfine structure measurement [19] was presented here. The half-life of the observed isomeric state with a firm spin-parity assignment,  $5/2^+$ , is estimated to be of the order of 10 ms, and we have seen no evidence of a controversial long-lived (5.8 s)

isomer under conditions where we would expect to clearly see it. Our non observation of this state is consistent with the conclusion from the recent measurement of the beta-decay of  $^{73}\text{Zn}$  [21] and also with the earlier  $\beta$ -decay study of  $^{73}\text{Cu}$  to  $^{73}\text{Zn}$  [22]. The recently reported abnormally large quadrupole moment for  $^{73}\text{Zn}$  [19] was reinvestigated by using shell model calculations with the JUN45 and A3DA-m interactions, and by a T-plot analysis which reveals a triaxial shape of the state. From the evolution of the orbital occupancies in the high-spin Zn states, an indispensable contribution of the  $E2$ -type excitation of both protons and neutrons in  $^{73m}\text{Zn}$  has been identified as the major reason for the large experimental quadrupole moment. This is further highlighted by the improved agreement observed with the A3DA-m shell model interaction, where additional proton excitations across the  $Z = 28$  closed shell and neutron excitations across the  $N = 50$  closed shell ( $E2$ -type excitations) occur. A T-plot analysis of the isomeric state in  $^{73}\text{Zn}$ , calculated from the MCSM basis states, suggests a triaxial shape for the  $5/2^+$  state in  $^{73}\text{Zn}$ . A systematic comparison with the adjacent even- and odd- $A$   $^{71-75}\text{Zn}$  isotopes shows that triaxial shapes also exist in the even- $A$   $^{72,74}\text{Zn}$ , but not in the odd- $A$   $^{71,75}\text{Zn}$ . Such triaxial deformations are already well known in the heavier even-even isotopes of Ge and Se in the same region, and are suggested in the region near  $Z = 43$ , where three quasiparticles in the  $g_{9/2}$  orbit can construct a  $5/2^+$  state. More experimental and theoretical investigations of the  $N = 43$  and  $Z = 43$  regions are necessary, such as laser spectroscopy studies of the nearby Ge and Se isotopes and also the analogical  $Z = 43$  (Tc) isotopes, for a better understanding of the abnormally large deformation and the related triaxiality.

#### ACKNOWLEDGMENTS

We acknowledge the support of the ISOLDE Collaboration and technical teams. The MCSM calculations were performed on the K computer at RIKEN AICS (hp150224, hp160211, hp170230). This work was supported by the National Key R&D Program of China (the High Precision Nuclear Physics Experiments), the HPCI Strategic Program (The Origin of Matter and the Universe) and ‘‘Priority Issue on post-K computer’’ (Elucidation of the Fundamental Laws and Evolution of the

Universe) from MEXT and JICFuS, the JSPS and FWO under the Japan-Belgium Research Cooperative Program the IAP-project P7/12, the FWO-Vlaanderen, GOA Grant No. 15/010 from KU Leuven, the NSF Grant No. PHY-1068217, the

BMBF Contract No. 05P15RDCIA, the Max-Planck Society, the Science and Technology Facilities Council, the Helmholtz International Center for FAIR (HIC for FAIR), and the EU FP7 via ENSAR No. 262010.

- [1] O. Sorlin, S. Leenhardt, C. Donzaud, J. Duprat, F. Azaiez, F. Nowacki, H. Grawe, Z. Dombradi, F. Amorini, A. Astier, D. Baiborodin, M. Belleguic, C. Borcea, C. Bourgeois, D. M. Cullen, Z. Dlouhy, E. Dragulescu, M. Gorska, S. Grevy, D. Guillemaud-Mueller, G. Hagemann, B. Herskind, J. Kiener, R. Lemmon, M. Lewitowicz, S. M. Lukyanov, P. Mayet, F. deOliveiraSantos, D. Pantalica, Y. E. Penionzhkevich, F. Pougheon, A. Poves, N. Redon, M. G. Saint-Laurent, J. A. Scarpaci, G. Sletten, M. Stanoiu, O. Tarasov, and C. Theisen, *Phys. Rev. Lett.* **88**, 092501 (2002).
- [2] R. Broda, B. Fornal, W. Krolas, T. Pawlat, D. Bazzacco, S. Lunardi, C. Rossi-Alvarez, R. Menegazzo, G. deAngelis, P. Bednarczyk, J. Rico, D. DeAcuna, P. J. Daly, R. H. Mayer, M. Sferazza, H. Grawe, K. H. Maier, and R. Schubart, *Phys. Rev. Lett.* **74**, 868 (1995).
- [3] C. Guenaut, G. Audi, D. Beck, K. Blaum, G. Bollen, P. Delahaye, F. Herfurth, A. Kellerbauer, H. J. Kluge, J. Libert, D. Lunney, S. Schwarz, L. Schweikhard, and C. Yazidjian, *Phys. Rev. C* **75**, 044303 (2007).
- [4] S. Rahaman *et al.*, *Eur. Phys. J. A* **34**, 5 (2007).
- [5] N. Aoi *et al.*, *Phys. Lett. B* **692**, 302 (2010).
- [6] C. J. Chiara, W. B. Walters, I. Stefanescu, M. Alcorta, M. P. Carpenter, B. Fornal, G. Gurdal, C. R. Hoffman, R. V. F. Janssens, B. P. Kay, F. G. Kondev, W. Krolas, T. Lauritsen, C. J. Lister, E. A. McCutchan, T. Pawlat, A. M. Rogers, D. Seweryniak, N. Sharp, J. Wrzesinski, and S. Zhu, *Phys. Rev. C* **84**, 037304 (2011).
- [7] O. Perru, O. Sorlin, S. Franchoo, F. Azaiez, E. Bouchez, C. Bourgeois, A. Chatillon, J. M. Daugas, Z. Dlouhy, Z. Dombradi, C. Donzaud, L. Gaudefroy, H. Grawe, S. Grevy, D. Guillemaud-Mueller, F. Hammache, F. Ibrahim, Y. LeCoz, S. M. Lukyanov, I. Matea, J. Mrazek, F. Nowacki, Y. E. Penionzhkevich, F. deOliveiraSantos, F. Pougheon, M. G. Saint-Laurent, G. Sletten, M. Stanoiu, C. Stodel, C. Theisen, and D. Verney, *Phys. Rev. Lett.* **96**, 232501 (2006).
- [8] C. Louchart *et al.*, *Phys. Rev. C* **87**, 054302 (2013).
- [9] Y. Toh, C. J. Chiara, E. A. McCutchan, W. B. Walters, R. V. F. Janssens, M. P. Carpenter, S. Zhu, R. Broda, B. Fornal, B. P. Kay, F. G. Kondev, W. Krolas, T. Lauritsen, C. J. Lister, T. Pawlat, D. Seweryniak, I. Stefanescu, N. J. Stone, J. Wrzesinski, K. Higashiyama, and N. Yoshinaga, *Phys. Rev. C* **87**, 041304(R) (2013).
- [10] J. Sun *et al.*, *Phys. Lett. B* **734**, 308 (2014).
- [11] T. D. Johnson, T. Glasmacher, J. W. Holcomb, P. C. Womble, S. L. Tabor, and W. Nazarewicz, *Phys. Rev. C* **46**, 516 (1992).
- [12] M. Niikura, B. Mougino, S. Franchoo, I. Matea, I. Stefan, D. Verney, F. Azaiez, M. Assie, P. Bednarczyk, C. Borcea, A. Burger, G. Burgunder, A. Buta, L. Caceres, E. Clement, L. Coquard, G. deAngelis, G. deFrance, F. deOliveiraSantos, A. Dewald, A. Dijon, Z. Dombradi, E. Fiori, C. Fransen, G. Friessner, L. Gaudefroy, G. Georgiev, S. Grevy, M. Hackstein, M. N. Harakeh, F. Ibrahim, O. Kamalou, M. Kmiecik, R. Lozeva, A. Maj, C. Mihai, O. Moller, S. Myalski, F. Negoita, D. Pantelica, L. Perrot, T. Pissulla, F. Rotaru, W. Rother, J. A. Scarpaci, C. Stodel, J. C. Thomas, and P. Ujic, *Phys. Rev. C* **85**, 054321 (2012).
- [13] S. Hellgartner, Ph.D. thesis, Technischen Universität München, 2015 (unpublished).
- [14] K. T. Flanagan, P. Vingerhoets, M. Avgoulea, J. Billowes, M. L. Bissell, K. Blaum, B. Cheal, M. DeRydt, V. N. Fedosseev, D. H. Forest, C. Geppert, U. Koster, M. Kowalska, J. Kramer, K. L. Kratz, A. Krieger, E. Mane, B. A. Marsh, T. Materna, L. Mathieu, P. L. Molkanov, R. Neugart, G. Neyens, W. Nortershauser, M. D. Seliverstov, O. Serot, M. Schug, M. A. Sjoedin, J. R. Stone, N. J. Stone, H. H. Stroke, G. Tungate, D. T. Yordanov, and Y. M. Volkov, *Phys. Rev. Lett.* **103**, 142501 (2009).
- [15] B. Cheal, E. Mane, J. Billowes, M. L. Bissell, K. Blaum, B. A. Brown, F. C. Charlwood, K. T. Flanagan, D. H. Forest, C. Geppert, M. Honma, A. Jokinen, M. Kowalska, A. Krieger, J. Kramer, I. D. Moore, R. Neugart, G. Neyens, W. Nortershauser, M. Schug, H. H. Stroke, P. Vingerhoets, D. T. Yordanov, and M. Zakova, *Phys. Rev. Lett.* **104**, 252502 (2010).
- [16] M. L. Bissell, T. Carette, K. T. Flanagan, P. Vingerhoets, J. Billowes, K. Blaum, B. Cheal, S. Fritzsche, M. Godefroid, M. Kowalska, J. Kramer, R. Neugart, G. Neyens, W. Nortershauser, and D. T. Yordanov, *Phys. Rev. C* **93**, 064318 (2016).
- [17] R. P. deGroote, J. Billowes, C. L. Binnersley, M. L. Bissell, T. E. Cocolios, T. DayGoodacre, G. J. Farooq-Smith, D. V. Fedorov, K. T. Flanagan, S. Franchoo, R. F. GarciaRuiz, A. Koszorus, K. M. Lynch, G. Neyens, F. Nowacki, T. Otsuka, S. Rothe, H. H. Stroke, Y. Tsunoda, A. R. Vernon, K. D. A. Wendt, S. G. Wilkins, Z. Y. Xu, and X. F. Yang, *Phys. Rev. C* **96**, 041302(R) (2017).
- [18] X. F. Yang, C. Wraith, L. Xie, C. Babcock, J. Billowes, M. L. Bissell, K. Blaum, B. Cheal, K. T. Flanagan, R. F. GarciaRuiz, W. Gins, C. Gorges, L. K. Grob, H. Heylen, S. Kaufmann, M. Kowalska, J. Kraemer, S. Malbrunot-Ettenauer, R. Neugart, G. Neyens, W. Nortershauser, J. Papuga, R. Sanchez, and D. T. Yordanov, *Phys. Rev. Lett.* **116**, 182502 (2016).
- [19] C. Wraith *et al.*, *Phys. Lett. B* **771**, 385 (2017).
- [20] E. Runte *et al.*, *Nucl. Phys. A* **441**, 237 (1985).
- [21] M. Huhta, P. F. Mantica, D. W. Anthony, P. A. Lofy, J. I. Prisciandaro, R. M. Ronningen, M. Steiner, and W. B. Walters, *Phys. Rev. C* **58**, 3187 (1998).
- [22] V. Vedia, V. Pazy, L. M. Fraile, H. Mach, W. Walters, A. Aprahamian, C. Bernards, J. A. Briz, B. Bucher, C. J. Chiara, Z. Dlouhy, I. Gheorghe, D. Ghita, P. Hoff, J. Jolie, U. Koster, W. Kurcewicz, R. Lica, N. Marginean, R. Marginean, B. Olaizola, J. M. Regis, M. Rudigier, T. Sava, G. S. Simpson, M. Stanoiu, and L. Stroe, *Phys. Rev. C* **96**, 034311 (2017).
- [23] M. Honma, T. Otsuka, T. Mizusaki, and M. Hjorth-Jensen, *Phys. Rev. C* **80**, 064323 (2009).
- [24] Y. Tsunoda, T. Otsuka, N. Shimizu, M. Honma, and Y. Utsuno, *Phys. Rev. C* **89**, 031301 (2014).

- [25] T. Togashi, Y. Tsunoda, T. Otsuka, and N. Shimizu, *Phys. Rev. Lett.* **117**, 172502 (2016).
- [26] R. Neugart *et al.*, *J. Phys. G: Nucl. Part. Phys.* **44**, 064002 (2017).
- [27] U. Köster, *Eur. Phys. J. A* **15**, 255 (2002).
- [28] V. N. Fedosseev *et al.*, *Rev. Sci. Instrum.* **83**, 02A903 (2012).
- [29] H. Franberg *et al.*, *Nucl. Instrum. Methods B* **266**, 4502 (2008).
- [30] U. Köster *et al.*, in *Nuclear Fission and Fission-Product Spectroscopy, 3rd International Workshop, May 2005, Cadarache, France*, edited by H. Goutte, H. Faust, G. Fioni, and D. Goutte, AIP Conf. Proc. No. 798 (AIP, New York, 2005), p. 315.
- [31] B. Erdal *et al.*, *Nucl. Phys. A* **194**, 449 (1972).
- [32] B. Cheal and K. T. Flanagan, *J. Phys. G: Nucl. Part. Phys.* **37**, 113101 (2010).
- [33] K. L. Heyde, *The Nuclear Shell Model*, 2nd ed. (Springer-Verlag, Berlin, 1994).
- [34] T. Otsuka, T. Suzuki, R. Fujimoto, H. Grawe, and Y. Akaishi, *Phys. Rev. Lett.* **95**, 232502 (2005).
- [35] T. Otsuka, T. Suzuki, M. Honma, Y. Utsuno, N. Tsunoda, K. Tsukiyama, and M. Hjorth-Jensen, *Phys. Rev. Lett.* **104**, 012501 (2010).
- [36] A. Welker, N. A. S. Althubiti, D. Atanasov, K. Blaum, T. E. Cocolios, F. Herfurth, S. Kreim, D. Lunney, V. Manea, M. Mougeot, D. Neidherr, F. Nowacki, A. Poves, M. Rosenbusch, L. Schweikhard, F. Wienholtz, R. N. Wolf, and K. Zuber, *Phys. Rev. Lett.* **119**, 192502 (2017).
- [37] C. Petrone *et al.*, INTC Document, ISOLDE-CERN, 2017 (unpublished).
- [38] L. Guo, J. A. Maruhn, and P.-G. Reinhard, *Phys. Rev. C* **76**, 034317 (2007).
- [39] N. Yoshinaga and K. Higashiyama, *J. Phys. Conf. Ser.* **445**, 012032 (2013).
- [40] G. H. Bhat, W. A. Dar, J. A. Sheikh, and Y. Sun, *Phys. Rev. C* **89**, 014328 (2014).
- [41] M. Lettmann *et al.*, *Phys. Rev. C* **96**, 011301(R) (2017).
- [42] S. Hu *et al.*, *Phys. Lett. B* **732**, 59 (2014).
- [43] B. Cheal *et al.*, *Phys. Lett. B* **645**, 133 (2007).
- [44] B. Cheal, K. Baczyńska, J. Billowes, P. Campbell, F. C. Charwood, T. Eronen, D. H. Forest, A. Jokinen, T. Kessler, I. D. Moore, M. Reponen, S. Rothe, M. Ruffer, A. Saastamoinen, G. Tungate, and J. Aysto, *Phys. Rev. Lett.* **102**, 222501 (2009).
- [45] F. Flavigny *et al.*, *Phys. Rev. Lett.* **118**, 242501 (2017).
- [46] P. Campbell, H. L. Thayer, J. Billowes, P. Dendooven, K. T. Flanagan, D. H. Forest, J. A. R. Griffith, J. Huikari, A. Jokinen, R. Moore, A. Nieminen, G. Tungate, S. Zemlyanoi, and J. Aysto, *Phys. Rev. Lett.* **89**, 082501 (2002).
- [47] S. Naimi, G. Audi, D. Beck, K. Blaum, C. Böhm, C. Borgmann, M. Breitenfeldt, S. George, F. Herfurth, A. Herlert, M. Kowalska, S. Kreim, D. Lunney, D. Neidherr, M. Rosenbusch, S. Schwarz, L. Schweikhard, and K. Zuber, *Phys. Rev. Lett.* **105**, 032502 (2010).
- [48] Y. X. Luo *et al.*, *J. Phys. G: Nucl. Part. Phys.* **31**, 1303 (2005).